

Proton NMR study of diffusion in continuous, nonstoichiometric metal-hydrogen systems: HfV₂H_x and ZrV₂H_x

J. Shinar

The Solid State Institute, The Technion—Israel Institute of Technology, Haifa 32000, Israel

D. Davidov and D. Shaltiel

Racah Institute of Physics and Energy Center, The Hebrew University, Jerusalem 91000, Israel

(Received 19 December 1983; revised manuscript received 18 June 1984)

The proton spin-relaxation times T_1 and T_2 in the continuous, nonstoichiometric, single-phase hydrides ZrV₂H_x and HfV₂H_x ($0.25 \leq x \leq 4.2$) were measured in the temperature range $100 \text{ K} \leq T \leq 500 \text{ K}$ at 10.7, 33.0, and 51.95 MHz. T_1 exhibits a minimum versus $1/T$ as well as asymmetry about this minimum. This asymmetry manifests itself mainly at low hydrogen concentrations ($x \leq 2.0$) but is noticeable up to $x = 3.5$. Although there are some differences in the behavior of the HfV₂H_x and ZrV₂H_x systems at low hydrogen concentrations ($x \leq 2.0$), at higher ones ($x > 2.0$) the behavior is similar. The temperature and frequency dependence of T_1 —and the asymmetry around the minimum in particular—are analyzed in terms of fluctuations of the dipolar interaction at the thermally activated hopping rate. This hopping rate is assumed to be governed by a *distribution* of activation energies. Good agreement with the experimental results is obtained. The “average” activation energy E_{a0} generally increases with x , from about 1000 K at $x = 0$ to about 5000 K at $x = 4$. The relative width of the distribution $\Delta E_a/E_{a0}$ decreases with x above $x = 2$. The logarithm of the “average” preexponential factor, $\ln \nu_0$, is found to be linear in E_{a0} , $\ln \nu_0 = \ln \nu_{00} + \beta E_a$. The intercept is $\nu_{00} = 1.66 \times 10^9 \text{ sec}^{-1}$ and the slope $\beta = 3.09 \times 10^{-3} \text{ K}^{-1}$. According to the model of Wert and Zener (WZ), β is the temperature derivative of the relative shear modulus $d(\mu/\mu_0)/dT$. However, the present value is larger than the value of $d(\mu/\mu_0)/dT$ observed for interstitial diffusion of various ions in transition metals. This point is discussed. In addition, according to the WZ model, ν_{00} is the hopping coordination number times the proton vibration frequency. The present value, $1.66 \times 10^9 \text{ sec}^{-1}$, is obviously too low to be interpreted as such. The solution of this problem, which has appeared in many disordered systems, is believed to be related to local concentration gradients and/or strain fields. These inhomogeneities apparently decrease (consequently causing the rapid rise of ν_0 and E_{a0}) as the concentration increases towards the quasistoichiometric limit $x = 4$.

I. INTRODUCTION

Many intermetallic compounds readily absorb large quantities of hydrogen to form ternary hydrides at ambient temperatures and pressures.^{1–6} Usually the formation of the hydrides is accompanied by a first-order phase transition from the hydrogen-poor so-called α phase to a new hydrogen-rich metal-hydride phase (the β phase). The first order $\alpha \rightarrow \beta$ phase transition manifests itself, for example, by the existence of a “plateau” region in the pressure-composition isotherms of these hydrides for temperatures and pressures smaller than a critical temperature, and pressure, respectively. In this region of constant temperature and pressure the two phases coexist in equilibrium. Above the critical temperature the transition to the hydrided β phase is a continuous one. The critical temperature for most of the metal-hydrogen systems is high above room temperature and consequently one can easily detect the precipitated β phase for temperatures in the vicinity of room temperature or lower using several experimental techniques, e.g., x-ray diffraction,⁴ neutron scattering,⁴ and Mössbauer measurements.⁷ Thus, no new information may be obtained by performing a systematic study as a function of hydrogen concentration on hydrides

in which phase separation occurs. This is one of the reasons that most of the NMR studies to date are restricted to the very limited concentration range in the α phase or the β phase. The cubic Laves phase (C15) compounds ZrV₂ and HfV₂ are apparently exceptions to this behavior. These metal compounds absorb large quantities of hydrogen,² yet no measured isotherm exhibits a plateau region. In addition, room-temperature x-ray diffraction measurements performed on HfV₂H_x, ZrV₂H_x, and Zr_{0.5}Hf_{0.5}V₂H_x hydrides^{2,8} show a continuous change of the lattice constants as a function of x , indicating a homogeneous phase at all concentrations (up to $x = 4.5$) (see Fig. 1). Other evidence is provided by room-temperature measurements of the V⁵¹ quadrupole splittings in ZrV₂H_x (Ref. 9) and HfV₂H_x (Ref. 10) and the continuous suppression of superconductivity in HfV₂H_x (Ref. 11) and Zr_{0.5}Hf_{0.5}V₂H_x (Ref. 8) up to $x = 1.5$ (this, indeed, indicates a homogeneous phase in these systems, up to $x = 1.5$, at liquid-helium temperatures).

In view of these properties, ZrV₂H_x and HfV₂H_x are obviously attractive for microscopic investigations. The interstitial sites occupied by the protons at room temperature have been determined by a series of neutron diffraction measurements^{12,13} to be the g site up to about $x = 2$

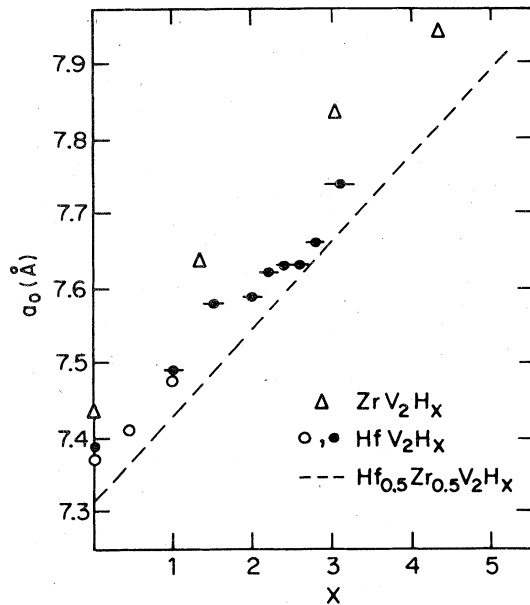


FIG. 1. Lattice constants of fcc (C15) $(\text{Hf,Zr})\text{V}_2\text{H}_x$ as a function of hydrogen concentration x . Open triangles are results of Pebler and Gulbransen on ZrV_2H_x (Ref. 2); open and solid circles the results of Duffer *et al.* (Ref. 11) and this work, respectively, on HfV_2H_x . The dashed line is the lattice constant of $\text{Hf}_{0.5}\text{Zr}_{0.5}\text{V}_2\text{H}_x$ as indicated by Rao *et al.* (Ref. 8).

and both the g and e sites at higher concentrations. The available sites are shown in Fig. 2. This is in agreement with phenomenological models.^{14,15} Quadrupole measurements of V^{51} NMR are also consistent with this picture.^{9,10} Thermal desorption spectroscopy measurements are also in agreement with this site occupation scheme and they further show that the bonding energy of protons in the concentration range $1 \leq x \leq 2.5$ is lower than for $x \leq 1$ although the protons occupy only the g site up to $x = 2.5$.¹⁶

This work concentrates mainly on the hydrogen diffusion properties as determined from the proton spin-relaxation rates. The model used to analyze the results is an adaptation of the modified Bloembergen-Purcell-Pound (BPP) theory^{17,18} developed by Walstedt *et al.*¹⁹ (which treats nuclear quadrupole interactions with fluctuations of the electric field gradient governed by a distribution of activation energies) to the case of fluctuating dipolar interactions. Indeed, it should not be surprising to find that the self-diffusion in the disordered ZrV_2H_x and HfV_2H_x systems—wherein the protons partially occupy the interstitial sites at random—is governed by a distribution of activation energies.

Following a description of the experimental procedure in Sec. II, the experimental results are described in Sec. III. A description of the model and the analysis of the results are given in Sec. IV. Usual analyses of this kind yield the activation energies (E_a 's) and preexponential factors (A_0 's) resulting from the assumption of a hopping rate satisfying the Arrhenius relation. In the present work this analysis also yields a linear relation between the E_a 's

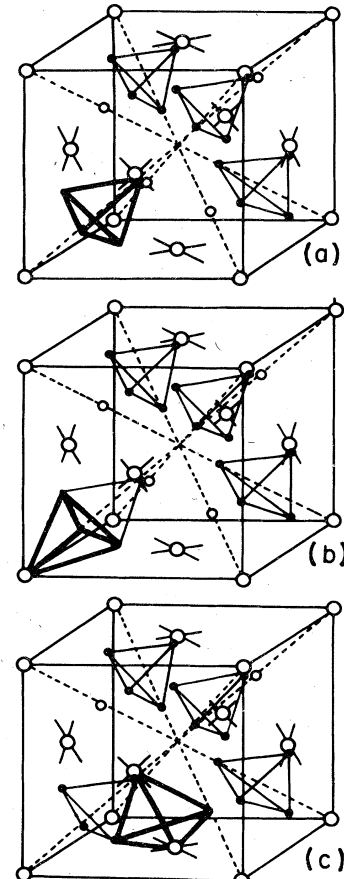


FIG. 2. Tetrahedral interstitial sites (IS's) in the Laves phase, fcc C15, AB_2 structure. Open circles are A atoms, solid circles are B atoms. (a) The b site—1 IS per formula unit, (b) the e site—4 IS's per formula unit, (c) the g site—12 IS's per formula unit.

and logarithms of A_0 's in the Arrhenius-like hopping rates governed by a distribution of E_a 's.

II. EXPERIMENTAL PROCEDURE

A. Sample preparation and x-ray study

Samples of HfV_2 and ZrV_2 were prepared by arc-melting 99.9% pure Hf clippings with 99.7% pure vanadium wire in an argon atmosphere. The resulting "buttons" of ZrV_2 were sealed in quartz tubes in about 100 mm Hg of argon and annealed for 24 h at 1175°C. In the case of HfV_2 annealing was unnecessary. X-ray diffraction measurements revealed about 97–99% cubic Laves phase. The powdered samples (about 0.5 g, grain size less than 100 μm) were then placed in a Pyrex reactor, degassed at 375°C for about 10–30 min and then hydrogenated to the desired concentration. The amount of hydrogen absorption was measured by the decrease of the pressure in the reactor chamber. The hydrided samples were cooled to 77 K (at which the proton diffusion is very slow), the pressure in the reactor was reduced to a few millimeters of Hg and the sample was sealed off with a gas flame. This ensured the nominal concentration of hydrogen in the sample at all times. In order to insure the phase homogeneity of the low-hydrogen-concentration

samples, these were also annealed at several hundred degrees centigrade after the hydrogenation.

As a check on the hypothesis of the phase homogeneity of the $\text{HfV}_2\text{-H}$ system, x-ray diffraction spectra of several hydride samples were taken at room temperature. However, due to experimental limitations, the samples were exposed to air during the diffraction measurement. All the spectra exhibited the fcc C15 structure. The lattice constants as determined from these spectra are shown in Fig. 1 as a function of hydrogen concentration. The spectra of $\text{HfV}_{1.5}$ and HfV_2H_2 revealed an additional weak spectrum of the hydrogen-free compound.

B. Proton relaxation times

Proton NMR spin-echo T_1 and T_2 measurements at 33 MHz were performed at the Hebrew University in Jerusalem and obtained from a single-frequency Spin-Lock CP-2 spectrometer coupled to a home-built pulse programmer and an on-line computer for data processing. The spin-spin dephasing time T_2 was obtained from the amplitude of the echo $A(t)$ at $t=2\tau$ following a $90^\circ\text{-}\tau\text{-}180^\circ$ pulse sequence. At temperatures sufficiently high for the diffusional narrowing to be considerable, the homogeneous part of the line shape is very nearly Lorentzian so that $A(t) = A_0 \exp(-t/T_2)$. However, at very high diffusion rates T_2 is effected by local magnetic field gradients and the results obtained using this method yield a decay constant nearly temperature independent, which is different from the true T_2 .¹⁸ Thus, our T_2 measurements were limited to a narrower temperature range than those of T_1 . The spin-lattice relaxation times T_1 were measured by applying one or several pulses which saturate the spin system, followed after a time t by either a single 90° or a $90^\circ\text{-}\tau_0\text{-}180^\circ$ pulse sequence. In most cases, the amplitude of the spin-echo or free-induction decay (FID) could be fitted well to the formula $M(t) = M_0[1 - A_1 \exp(-t/T_1)]$ where $1 \leq A_1 \leq 2$. However, in certain cases nonexponential relaxation was observed, and served, and is described in the next section. T_1 measurements at other frequencies (mostly through saturation of the FID) were obtained from a home-built spectrometer at the Solid State Institute and Physics Department of the Technion, Haifa. Nonexponential relaxation could not be resolved in this system—probably due to instrumental limitations.

III. EXPERIMENTAL RESULTS

A. Low hydrogen concentrations (HfV_2H_x and ZrV_2H_x , $x \leq 2$)

The results of the spin-relaxation measurements in HfV_2H_x and ZrV_2H_x in concentrations $x \leq 2$ are shown in Figs. 3–7. T_2 decreases as a function of the temperature T . It has a roughly logarithmic dependence on $1/T$ except at high temperatures, where the spin-echo measured values are effected by local magnetic field gradients (as mentioned in the preceding section) and as a result deviate from this logarithmic dependence on $1/T$. However, it should be noted that in ZrV_2H_x , $x=0.25$ and 0.5 ,

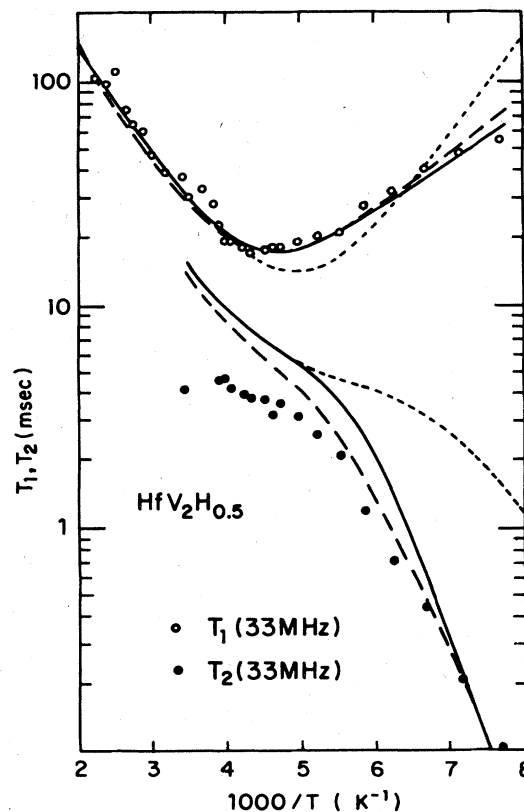


FIG. 3. Proton spin-spin relaxation time T_2 and spin-lattice relaxation time T_1 at 33 MHz in $\text{HfV}_2\text{H}_{0.5}$. The dotted line is the fit of the model described in Sec. IV with zero distribution width of the activation energy E_a . The dashed line is the fit using a relative Lorentzian distribution width $\Delta E_a/E_{a0}=0.135$ and the quadratic relation [Eq. (12)] between the preexponential A_0 and E_a . The solid line is the prediction of the model using a relative width $\Delta E_a/E_{a0}=0.21$ and the Zener relation [Eq. (13)] between A_0 and E_a . See also Table I.

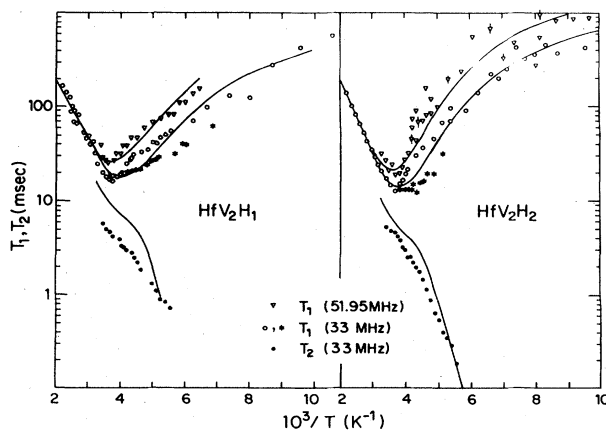


FIG. 4. Proton spin-relaxation times in HfV_2H_1 and HfV_2H_2 . The open circles are the values of the spin-echo T_1 at 33 MHz using a small value of the delay time τ_0 in the $90^\circ\text{-}180^\circ$ pulse sequence, about $30 \mu\text{sec}$, and the asterisks are the values obtained when τ_0 is long, about $300 \mu\text{sec}$ (see Fig. 8). The solid lines are the predictions of the model described in Sec. IV using the parameters listed in Table I.

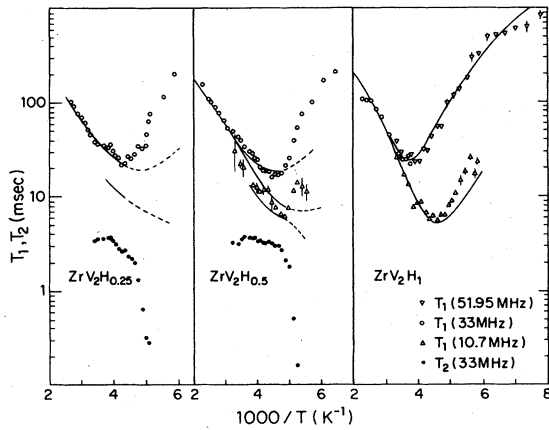


FIG. 5. Proton spin-relaxation times in ZrV_2H_x , $x=0.25, 0.5, 1$. The lines are the predictions of the model described in Sec. IV using the parameters given in Table I.

the slope of $\ln T_2$ versus $1/T$ is anomalously high. This will be discussed in the next sections.

In all cases, there is a clear minimum in T_1 versus $1/T$, the position and value of which is frequency dependent. This clearly indicates that the dominant relaxation mechanism is the dipolar interaction obviously fluctuating at the hopping rate (see Sec. IV below). However, the clearly asymmetric behavior (nonequal slopes) of $\ln T_1$ around this minimum and the "flattening off" of T_1 at low temperatures indicate complex, non-Arrhenius-like behavior (see Sec. IV). In ZrV_2H_x , $x=0.25$ and 0.5 , the low- T slope is higher than the high- T one. In all other cases in ZrV_2H_x and HfV_2H_x the high- T slope is higher. Another characteristic is the larger slopes (activation energies, see below) in ZrV_2H_x ($x=1.0, 1.4$, and especially $1.5, 1.6$, and 1.75) as compared to HfV_2H_x $x=0.5, 1.0$, and 2 .

Interesting behavior was observed in measuring T_1 in HfV_2H_1 and HfV_2H_2 in the temperature range $180 \leq T \leq 260$ K. The recovery of the proton spin-echo magnetization $M(t)$ towards asymptotic value M_0 as a

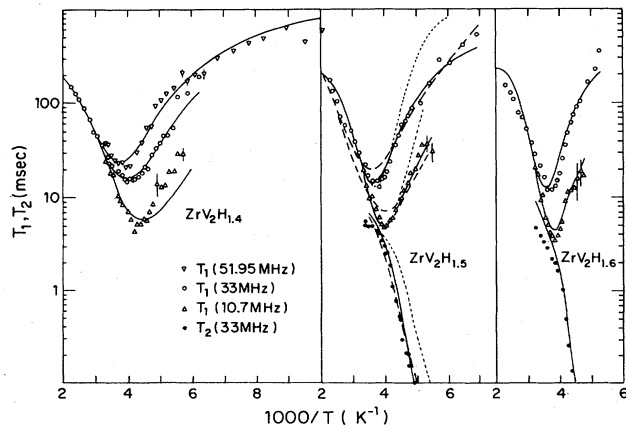


FIG. 6. Proton spin-relaxation times in ZrV_2H_x , $x=1.4, 1.5, 1.6$. The lines are the predictions of the various models as described in the caption of Fig. 3 and in Sec. IV. The parameters used to produce the solid lines are given in Table I.

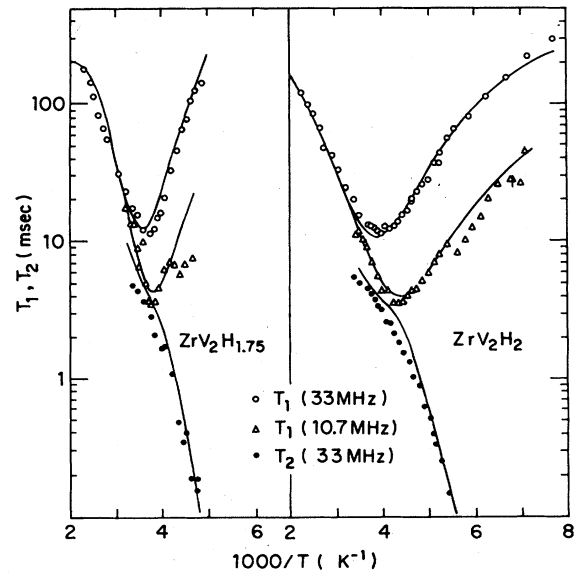


FIG. 7. Proton spin-relaxation times in ZrV_2H_x , $x=1.75, 2$. The lines are the predictions of the model described in Sec. IV using the parameters listed in Table I.

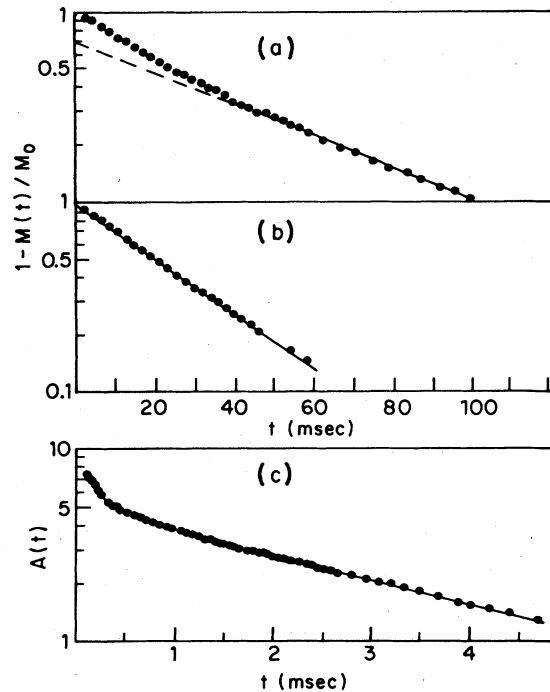


FIG. 8. Nonexponential relaxation in HfV_2H_1 and HfV_2H_2 . (a) Recovery of proton spin-echo magnetization $M(t)$ towards the asymptotic value M_0 as a function of the separation time t between the saturating pulse train and the 90° - τ_0 - 180° pulse sequence. In this case $\tau_0=20.1 \mu\text{sec}$. Note the deviation from single exponential recovery which is a straight line on this logarithmic scale. (b) Same as in (a), except $\tau_0=550 \mu\text{sec}$. Note the simple exponential recovery in this case. (c) Proton spin-echo amplitude $A(t)$ vs separation t between 90° and 180° pulses. Note the deviation from exponential decay at small values of t . These relaxations were observed in HfV_2H_1 at 210 K.

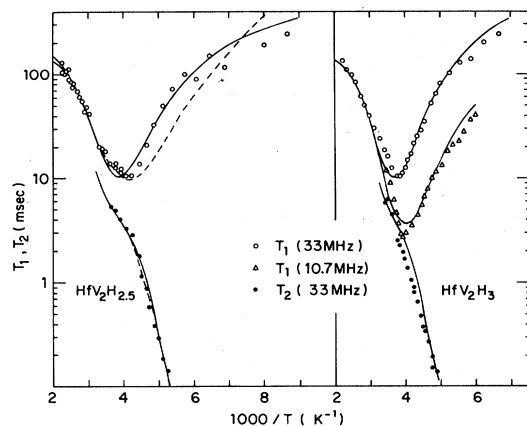


FIG. 9. Proton spin-relaxation times in $\text{HfV}_2\text{H}_{2.5}$ and HfV_2H_3 . The lines are the predictions of the various models as described in the caption of Fig. 3 and in Sec. IV. The parameters used to produce the solid lines are listed in Table I.

function of the separation time t between the saturating pulse train and the 90° - τ_0 - 180° pulse sequence was nonexponential when τ_0 was short [$\leq 30 \mu\text{sec}$; see Fig. 8(a)]. In this case, the T_1 values shown as open circles in Fig. 4 were obtained from the long t tail of the recovery. The recovery approached exponential behavior as τ_0 was increased, but the values of T_1 extracted from the tail of the recovery decreased, as can be seen from the difference in the slopes in Figs. 8(a) and 8(b) [in Fig. 8(b), $\tau_0 = 550 \mu\text{sec}$]. Shown in Fig. 4 are the largest and smallest values of T_1 obtained using the different values of τ_0 .

B. High concentrations (HfV_2H_x and ZrV_2H_x , $x > 2$)

The relaxation rates at high concentrations are shown in Figs. 9–12. The major features are as follows:

- (1) The behavior of ZrV_2H_x is similar to HfV_2H_x in

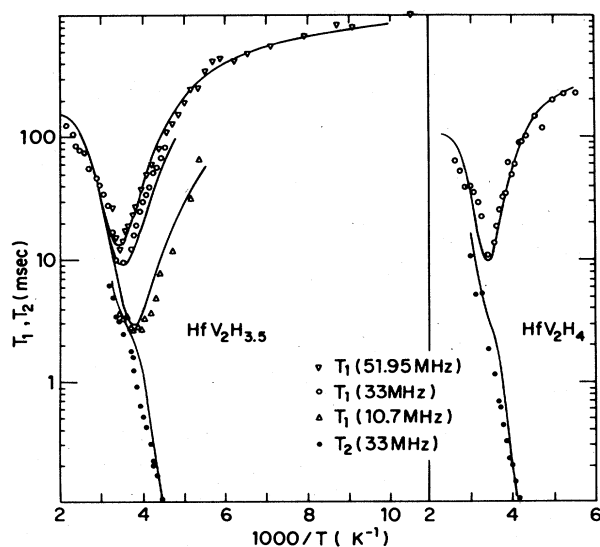


FIG. 10. Proton spin-relaxation times in $\text{HfV}_2\text{H}_{3.5}$ and HfV_2H_4 . The lines are the predictions of the model described in Sec. IV using the parameters listed in Table I.

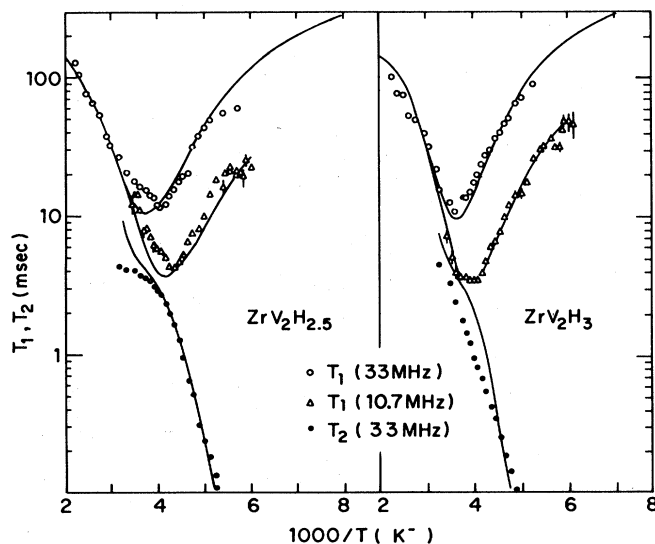


FIG. 11. Proton spin-relaxation times in $\text{ZrV}_2\text{H}_{2.5}$ and ZrV_2H_3 . The lines are the predictions of the model described in Sec. IV using the parameters listed in Table I.

this concentration range, in contrast to the differences at lower concentrations.

- (2) The asymmetry of the slopes of $\ln T_1$ around the minimum decreases as x increases. The values of the slopes rapidly increase up to $x = 4$.

- (3) The slope of $\ln T_1$ versus $1/T$ flattens off at low T .

- (4) The relaxation rates in $\text{ZrV}_2\text{H}_{4.2}$ differ sharply from those in ZrV_2H_4 , an indication that $x = 4$ is a quasi-stoichiometric concentration, in accordance with observations and predictions^{14–16} by others.

IV. ANALYSIS

A. Model equations

Clearly, the dominant spin-lattice relaxation mechanism in our case is the dipolar coupling modified by the

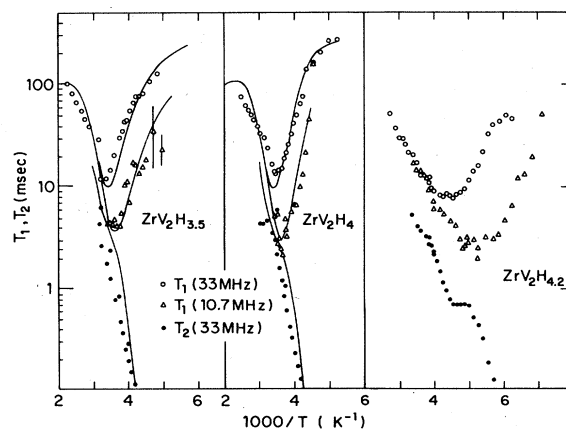


FIG. 12. Proton spin-relaxation times in ZrV_2H_x , $x = 3.5, 4, 4.2$. The lines are the predictions of the model described in Sec. IV using the parameters listed in Table I. Note the broadening of the minimum in $x = 4.2$ as compared to $x = 4$.

proton diffusion. The spin-lattice and spin-spin relaxation rates due to the coupling between like spins are then given by¹⁸

$$1/T_1 = \frac{3}{2} \gamma^u \hbar^2 I(I+1) [J_2(2\omega) + J_1(\omega)], \quad (1a)$$

$$1/T_2' = \frac{4}{9} \gamma^u \hbar^2 I(I+1) \left[\frac{3}{8} J_2(2\omega) + \frac{15}{4} J_1(\omega) + \frac{3}{8} J_0(0) \right], \quad (1b)$$

where

$$J_k(\omega) = \int_{-\infty}^{\infty} e^{i\omega t} \sum_j \langle F_{ij}^{(k)}(t') F_{ij}^{(k)*}(t'+t) \rangle_{\text{Av}(t')} dt \quad (2)$$

($k=1,2$) are the spectral densities of the time correlation functions of the various terms in the fluctuating dipolar Hamiltonian:

$$F_{ij}^{(1)}(t) = \sin\theta_{ij} \cos\theta_{ij} e^{i\phi_{ij}} / r_{ij}^3, \quad (3a)$$

$$F_{ij}^{(2)}(t) = \sin^2\theta_{ij} e^{2i\phi_{ij}} / r_{ij}^3. \quad (3b)$$

It is usually assumed that the correlation functions decay exponentially at the hopping rate $\tau^{-1} = \nu$ which obeys an Arrhenius relation

$$\nu = A_0 e^{-E_a/kT}, \quad (4)$$

where A_0 is the preexponential factor and E_a is the activation energy (the enthalpy of motion²⁰). Under these conditions the integrals in Eqs. (2) yield the following expression for the proton dipolar contribution to the relaxation rates $1/T_{1H}$ and $1/T_{2H}'$ (see, e.g., Abragam¹⁸):

$$1/T_{1H} = \frac{2}{3} \frac{\gamma^2}{\omega} M_{2H} \left[\frac{y}{1+y^2} + \frac{4y}{1+4y^2} \right], \quad (5a)$$

$$1/T_{2H}' = \frac{4}{9} \frac{\gamma^2}{\omega} M_{2H} \left[\frac{3}{2} \frac{y}{1+4y^2} + \frac{15}{4} \frac{y}{1+y^2} + \frac{9}{4} y \right], \quad (5b)$$

where ω is the Larmor frequency, $y = \omega\tau$ and

$$M_{2H} = \frac{3}{5} \gamma^2 \hbar^2 I(I+1) \sum_j r_{ij}^{-6} \quad (6)$$

is the contribution to the rigid-lattice second moment from like spins (the summation being over all sites occupied by protons). In the case of HfV_2H_x and ZrV_2H_x , one should also add the contribution to the relaxation from the unlike V^{51} ($I = \frac{7}{2}$) spins:

$$1/T_{1V} = \frac{\gamma^2}{\omega} M_{2V} \left[\frac{1}{2} \frac{y}{1+(1-\gamma_V/\gamma_H)^2 y^2} + \frac{3}{2} \frac{y}{1+y^2} + 3 \frac{y}{1+(1+\gamma_V/\gamma_H)^2 y^2} \right], \quad (7a)$$

$$1/T_{2V}' = \frac{\gamma^2}{\omega} M_{2V} \left[y + \frac{1}{4} \frac{y}{1+(1-\gamma_V/\gamma_H)^2 y^2} + \frac{3}{4} \frac{y}{1+y^2} + \frac{3}{2} \frac{y}{1+(\gamma_V/\gamma_H)^2 y^2} + \frac{3}{2} \frac{y}{1+(1+\gamma_V/\gamma_H)^2 y^2} \right], \quad (7b)$$

where

$$M_{2V} = \frac{4}{15} \gamma_V^2 \hbar^2 I_V(I_V+1) \sum_j r_{ij}^{-6}. \quad (8)$$

γ_V being the V^{51} gyromagnetic ratio and the summation is over the distances from a given proton to all V^{51} nuclei. The total relaxation rates $1/T_{10}$ and $1/T_{20}'$ are then given by

$$1/T_{10} = 1/T_{1H} + 1/T_{1V}, \quad (9a)$$

$$1/T_{20}' = 1/T_{2H}' + 1/T_{2V}'. \quad (9b)$$

From Eqs. (5), (7), and (9) one can easily see that when $\omega\tau \ll 1$ (extreme motional narrowing), $1/T_{20}' = 1/T_{10}$. When $\omega\tau \gg 1$ (but still in the motionally narrowed regime) only the terms directly proportional to y in Eqs. (5b) and (7b) contribute significantly to $1/T_{20}'$ and therefore $\ln T_{20}'$ is linear in $1/T$ with a slope equal to E_a/k .

Using Eqs. (5a), (7a), and (9a) it can be shown that $1/T_{10}$ is maximal (T_{10} minimal) for some value y_0 of y which depends on the ratio M_{2H}/M_{2V} . In the extreme case where $M_{2V}=0$, $y_0=0.616$ and when $M_{2H}=0$, $y_0 \approx 0.9$. In all intermediate cases, $0.6 \leq y_0 \leq 0.9$ and T_{10} varies only slightly in this region.²¹ In temperature regions such that $y \gg 1$ or $y \ll 1$, $\ln T_1$ is linear in the inverse temperature $1/T$, with a slope whose absolute value is E_a/k . Yet the experimental results (Figs. 3–7 and 9–12) are at variance with a symmetric behavior of T_1 about the minimum. Therefore, the decay of the dipolar correlation functions [Eqs. (3)] cannot be characterized by a constant whose temperature dependence is a single Arrhenius one [Eq. (4)]. Therefore, the hopping rate cannot be characterized by an Arrhenius dependence with a single value of E_a . Yet neutron scattering studies and model calculations all suggest that at low concentrations (below 2.5 H atoms per formula unit) the protons all occupy equivalent g sites (Fig. 2). Since, however, the activation energy at a given site E_a is (at least partially) determined by self-trapping lattice strain fields induced by the interstitial H atoms,²² it should depend on the particular (but random) configuration of other H atoms in adjacent sites. This presents an intrinsic difference between interstitial diffusion in nonstoichiometric versus stoichiometric systems. The diffusion process is therefore expected to be governed by a *distribution* of activation energies according to the distribution of configurations around the various (but on the average equivalent) sites.

Our problem is therefore to evaluate the correlation functions

$$k_l(t) = \sum_j \langle F_{ij}^{(l)}(t') F_{ij}^{(l)*}(t'+t) \rangle_{\text{Av}(t')} \quad (10)$$

in the presence of fluctuations whose rate is determined by a distribution of E_a 's. Walstedt *et al.*¹⁹ have evaluated these expressions for the case of quadrupolar relaxation in the presence of similar fluctuations in the electric field gradients around Na^+ ions in $\text{Na-}\beta$ -alumina. The adaptation of the model to fluctuating dipolar fields is straightforward if for simplicity we assume that for each configuration $k_2(0) \approx 4k_1(0)$ [see Eqs. (3) and Refs. 18 and 23]. The resulting expression for the relaxation rate T_{1d}^{-1} is

then given by²⁴

$$T_{1d}^{-1} = \int dE_a G(E_a) T_{10}^{-1}(E_a, A_0), \quad (11a)$$

where $G(E_a)$ is a normalized distribution function with a distribution width ΔE_a . $1/T_2'$ is similarly given by

$$1/T_2' = \int dE_a G(E_a) T_{20}'^{-1}(E_a, A_0). \quad (11b)$$

It should be noted, however, that the measured spin-echo $1/T_2$ contains $1/T_2'$ and $1/T_{2d}$ processes so that²⁵

$$1/T_2 = 1/T_2' + 1/T_{2d}. \quad (12)$$

The distribution of activation energies has the following qualitative effects on the behavior of T_1 and T_2 . (a) The slope of $\ln T_1$ versus $1/T$ at temperatures below the minimum is smaller than the high-temperature one. (b) If the relative distribution width $\Delta E_a/E_{a0}$ (E_{a0} being the average E_a) is sufficiently large (≥ 0.2 for a Lorentzian distribution and ≥ 0.3 for a Gaussian one), then the calculated T_1 becomes almost temperature independent at very low temperatures. (c) If the relative distribution width is considerable (≥ 0.1 for Lorentzian, ≥ 0.15 for Gaussian), the calculated values of $\ln T_2$ below the temperature of the minimum in T_1 (but still in the motionally narrowed region) are no longer linear in $1/T$, and the slope of $\ln T_2$ increases as the temperature T decreases (i.e., "bends downward"). This last feature is easily observed in the measured values of T_2 in ZrV_2H_x , $1.4 \leq x \leq 1.6$ (see Fig. 6).

B. The dependence of A_0 on E_a

In solving Eqs. (11), the dependence of the preexponential factor A_0 given in Eq. (4) on E_a is still required. In fitting the similar equation to the results of the Na^{23} relaxation in superionic $\text{Na-}\beta\text{-Al}_2\text{O}_3$, Walstedt *et al.*¹⁹ chose a square-root dependence of A_0 on E_a :

$$A_0 = \nu_0 (E_a/E_{a0})^{1/2}. \quad (13)$$

This relation results from simple model theories on hopping over (rigid) sinusoidal potential barriers.²⁶ In effect, this square-root dependence is so weak as to be practically equivalent to an E_a independent A_0 .

During the initial fitting procedure between the model equations (11) and the experimental results, the square-root relation between A_0 and E_a was chosen. In some cases a fit to an E_a independent A_0 was also attempted. However, the results of the fitting procedure yielded, among the various samples of HfV_2H_x and ZrV_2H_x , a remarkably linear relation between the logarithm of the (average) preexponential factor and the average activation energy:

$$\ln \nu_0 = \ln \nu_{00} + \beta E_{a0}. \quad (14)$$

This linear relation extended over 6 orders of magnitude in A_0 , from about $8 \times 10^{10} \text{ sec}^{-1}$ in $\text{HfV}_2\text{H}_{0.5}$ to about 10^{17} sec^{-1} in HfV_2H_4 , yielding an intercept $\nu_{00} = 1.66 \times 10^9 \text{ sec}^{-1}$ and slope $\beta = 3.09 \times 10^{-3} \text{ K}^{-1}$.

Owing to the observed linear relation between $\ln \nu_0$ and E_{a0} [Eq. (14)], the model equations (11) were refitted to the experimental results, using, within each concentration,

this relation and the above-mentioned values of ν_{00} and β . Indeed, although the *same* values of ν_{00} and β were used for (almost) all concentrations, the obtained fits were, in some cases, actually better than during the square-root-dependent fitting procedure (see Fig. 6, and in particular, Fig. 9). Qualitatively, the calculated behavior of T_1 using the square-root relation [Eq. (13)] is much "flatter" around the minimum than that calculated using Eq. (14) with the given (large) value of β .

C. Comparison between theory and experimental results

The fits between the T_1 and T_2 data and the model, Eqs. (11), are given by the solid lines in Figs. 3 to 7 and 9 to 12. The model behavior was obtained using a Lorentzian distribution function and the linear relation [Eq. (14)] between $\ln A_0$ and E_a . The quality of the agreement was roughly the same for Gaussian and Lorentzian distributions. The model was fitted to the observed values by choosing, for each concentration, appropriate values of M_{2H} [Eq. (6)], M_{2V} , [Eq. (8)], and E_{a0} and ΔE_a [Eqs. (11)] to obtain a best fit. The minimal value of T_{1d} [Eq. (11a)] is determined by a linear combination of M_{2H} and M_{2V} which is about $0.9M_{2H} + 2.2M_{2V}^{1/2}$ (see below).

The observed values of T_2 deviate from the calculated ones at high temperatures, and are particularly noticeable at low hydrogen concentrations. This deviation of the spin-echo measured T_2 results from magnetic field gradients, and it is shorter than the true transverse relaxation time, as mentioned in Sec. II above.

The values of the average activation energies E_{a0} and Lorentzian distribution widths ΔE_a used to fit the model to the data in the various concentrations are listed in Table I. In the Zener model for interstitial diffusion,²⁰ ν_{00} [see Eq. (14)] is interpreted as $n\nu$, where n is the hopping coordination number and ν is the vibration frequency of the proton in its equilibrium site. The value of $n\nu$ is expected to be in the range $5 \times 10^{12} - 5 \times 10^{13} \text{ sec}^{-1}$, and therefore $\nu_{00} = 1.66 \times 10^9 \text{ sec}^{-1}$ is much too small to be interpreted as $n \times \nu$. The value of β , about $3 \times 10^{-3} \text{ K}^{-1}$, is large compared to those observed for heavy interstitials diffusing in various transition metals.²⁰ Yet these anomalous results do not invalidate the foregoing analysis. Indeed, anomalously low values of the preexponential invariably coupled to small values of E_a [thus conserving the Zener relation, Eq. (14), between them] have been observed in many previous cases.²⁷ The clarification of this problem is elaborated in Sec. V.

In several cases it was necessary to add a Korringa term¹⁸ to the total relaxation rate

$$1/T_{1e} = C_k T, \quad (15)$$

and the resulting values of C_k are also presented in Table I. The flattening off of $\ln T_1$ versus $1/T$ at *high* temperatures, observed in several samples (Figs 6, 7, and 9–12) are apparently due to the Korringa term. The analysis and discussion of the interaction between the proton spins and conduction electrons will, however, be deferred to a later work.

TABLE I. Average activation energies E_{a0} , distribution widths ΔE_a , average preexponentials ν_0 , and Korrington coefficients C_K used to fit the model Eq. (11) to the data. The preexponential A_0 is derived from the relation $A_0(E_a) = \nu_0 e^{\beta E_a}$ [Eq. (14)] where, in all cases, $\beta = 3.09 \times 10^{-3} \text{ K}^{-1}$ and, unless stated otherwise, $\nu_0 = 1.66 \times 10^9 \text{ sec}^{-1}$. The average preexponential ν_0 is given by $\nu_0 = \nu_{00} e^{\beta E_{a0}}$.

Concentration x	E_{a0} (K) $\pm 15\%$	E_a (K) $\pm 20\%$	ν_0 (sec^{-1})	C_K ($\text{sec K})^{-1}$
In HfV_2H_x				
0.5	1050.0	325.0	4.3×10^{10}	
1.0 ^a	1600.0	450.0	1.9×10^{11}	
2.0 ^b	2000.0	400.0	5.5×10^{11}	
2.5 ^c	2550.0	475.0	6.6×10^{12}	0.01
3.0	3100.0	525.0	2.4×10^{13}	0.0105
3.5 ^d	4000.0	650.0	3.9×10^{13}	0.0106
4.0	5800.0	800.0	1.0×10^{17}	0.02
In ZrV_2H_x				
0.25	1100.0	150.0	5.0×10^{10}	
0.5	1200.0	300.0	6.7×10^{10}	
1.0	1900.0	250.0	5.9×10^{11}	0.004
1.4	2000.0	400.0	8.0×10^{11}	0.004
1.5	3200.0	600.0	3.3×10^{13}	0.007
1.6	4100.0	750.0	5.3×10^{14}	0.007
1.75	3700.0	450.0	1.5×10^{14}	0.008
2.0	2200.0	450.0	1.5×10^{12}	0.005
2.5	2500.0	500.0	3.8×10^{12}	0.007
3.0	3300.0	600.0	4.5×10^{13}	0.01
3.5	5000.0	800.0	8.5×10^{15}	0.02
4.0	5400.0	500.0	2.9×10^{16}	0.02

^a $\nu_{00} = 1.4 \times 10^9 \text{ sec}^{-1}$.

^b $\nu_{00} = 1.2 \times 10^9 \text{ sec}^{-1}$.

^c $\nu_{00} = 2.5 \times 10^9 \text{ sec}^{-1}$.

^dIn this case a spin diffusion term $(1/T_1)_{\text{SD}} = 0.1 \text{ sec}^{-1}$ was also added.

TABLE II. Observed and calculated values of $0.9M_{2H} + 2.2M_{2V}$ [which determines $(T_{1d})_{\text{min}}$], assuming random occupation of nonadjacent g sites.

Concentration x	$0.9M_{2H} + 2.2M_{2V}$	
	Obs.	Calc. (G^2)
In HfV_2H_x		
0.5	23.0	24.0
1.0	22.0	27.0
2.0	26.0	33.0
2.5	34.0	37.0
3.0	35.0	38.0
3.5	38.0	40.0
4.0	36.0	42.0
In ZrV_2H_x		
0.25	18.0	22.0
0.5	21.0	23.0
1.0	23.0	26.0
1.4	25.0	28.0
1.5	28.0	29.0
1.6	28.0	30.0
1.75	33.0	30.0
2.0	33.0	32.0
2.5	34.0	36.0
3.0	36.0	37.0
3.5	33.0	38.0
4.0	33.0	40.0

Table II presents the values of the linear combination $0.9M_{2H} + 2.2M_{2V}$ used to fit the model to the data. Only that quantity is listed since, as mentioned above, it alone is determined by the minimal value of T_1 . In that table this linear combination is compared to the values calculated from Eqs. (6) and (8), assuming random occupation of nonadjacent g sites [as determined by neutron scattering measurements and model calculations^{12,14}] and the concentration dependent lattice parameters as determined by x-ray measurements (Fig. 1). The agreement between the observed and calculated values is reasonable. However, the observed values are, generally, somewhat lower. This may be due to the strain fields produced by the proton resulting in the local dilatation of the lattice as compared to the average values obtained from the x-ray measurements.

It should be noted that the calculated values of $0.9M_{2H} + 2.2M_{2V}$, assuming random occupation of *all* g sites or *all* g and e sites (i.e., including adjacent ones), are about 3 times larger than those listed in Table II. In other words, the relaxation measurements add strong (albeit indirect) evidence that the protons do not occupy adjacent sites.

The features resulting from the fit between the model [Eqs. (11)] and the data may be summarized as follows:

(1) The nonexponential relaxation in HfV_2H_1 and HfV_2H_2 (Fig. 8) may account for the discrepancies between the model and the observed values. The predicted

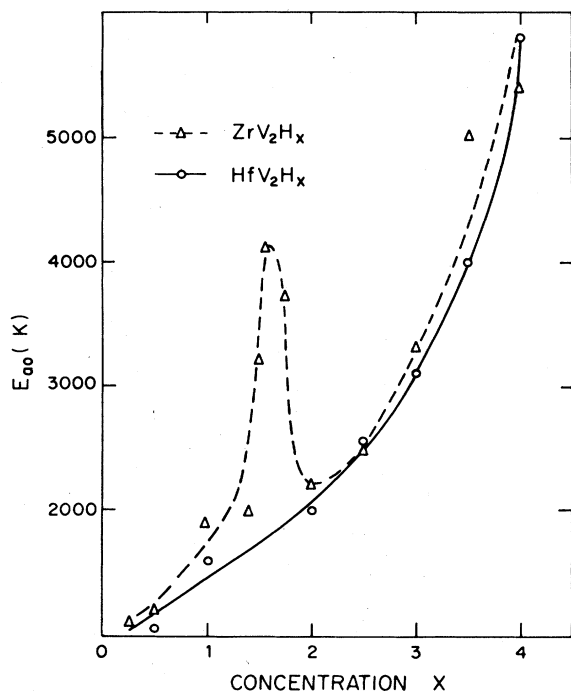


FIG. 13. The concentration x dependence of the average activation energy E_{a0} in HfV_2H_x and ZrV_2H_x . The lines are a guide to the eye.

values at 33 MHz lie between the observed extreme values (Fig. 4).

(2) It can be shown from the model Eqs. (11) that for all distribution widths $\Delta E_a \neq 0$ the low-temperature slope of $\ln T_1$ versus $1/T$ is smaller than the high-temperature one. This is in agreement with the observed behavior in all concentrations except $\text{ZrV}_2\text{H}_{0.25}$ and $\text{ZrV}_2\text{H}_{0.5}$, where the opposite is the case. Therefore, the asymmetry in these two cases must be due to a different reason. The sharp drop in T_2 in these concentrations around 200 K suggests a transition to a low-temperature phase in which hydrogen diffusion is slower. A neutron and/or x-ray diffraction study of these cases may help clarify this feature.

(3) In ZrV_2H_x there is an anomalous peak in E_{a0} at $x=1.6$, and the values in the range $1.0 \leq x \leq 1.75$ are very high (Fig. 13). These high activation energies hint to anomalously high hydrogen-induced self-trapping lattice strain fields (see this section above). The nature of this behavior is not understood at present.

(4) The close agreement between the observed positions of the minima in T_1 and the calculated ones justify the assumption of the Zener (linear) relation²⁰ between $\ln A_0$ and E_a . Indeed, this relation appears to be widespread among other ternary hydride systems (see Sec. V) as shown by Shinar *et al.*²⁸

(5) Another interesting result from the model fitting procedure is the concentration dependence of the average activation energy E_{a0} (Fig. 13). In thermally activated sinusoidal barrier hopping, E_{a0} is expected to be proportional to d^2 , where d is the jump distance.²⁶ However, in both ZrV_2H_x and HfV_2H_x , the lattice constant [and therefore the distance between adjacent g sites (see Fig. 2)] in-

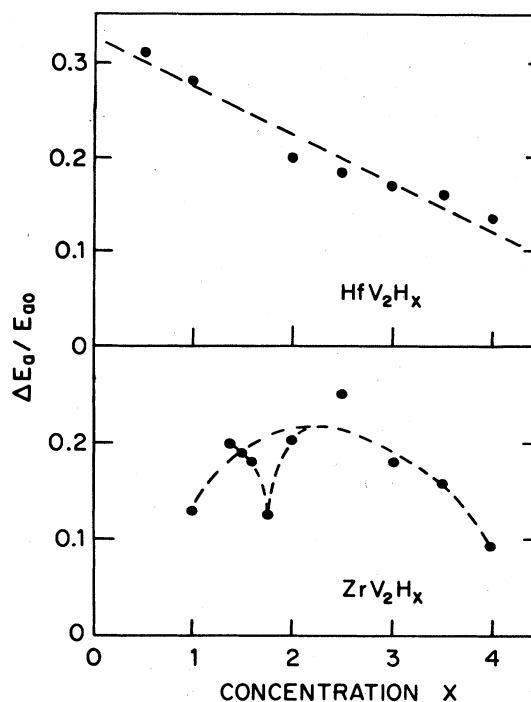


FIG. 14. The concentration x dependence of the relative Lorentzian width $\Delta E_a/E_{a0}$ of the activation energy distribution in HfV_2H_x and ZrV_2H_x . The lines are a guide to the eye.

creases by only 7% from $x=0$ to $x=4$. Yet E_{a0}/k changes by a factor of 6, from about 1000 K at $x=0.5$ to about 6000 K at $x=4$. Therefore, this disagreement eliminates the possibility of basing the analysis of the results on the interpretation of E_a as an even nearly sinusoidal potential barrier, as may be *a priori* suggested.

(6) In HfV_2H_x the relative width of the distribution of activation energies, $\Delta E_a/E_{a0}$, monotonically decreases as the proton concentration increases; in ZrV_2H_x , except for the dip in the region of anomalously high E_{a0} 's ($1.4 \leq x \leq 1.75$), it peaks below $x=2$ and decreases beyond (Fig. 14). *A priori*, one might expect the distribution width to peak when the occupancy of the nonadjacent g sites is 0.5 (i.e., when $x=2$). However, there are complicating factors which would probably influence the distribution width such as the concentration dependence of the bonding energy and the occupation of e sites at concentrations higher than $x=2.5$. Only the decrease of $\Delta E_a/E_{a0}$ beyond $x=3$ may intuitively be understood to result from the formation of a hydrogen superstructure at these high densities and low temperatures.^{12,13}

(7) An interesting feature of the results in ZrV_2H_x are the large changes in the relaxation times observed when the concentration is increased from ZrV_2H_4 to $\text{ZrV}_2\text{H}_{4.2}$. In this highest concentration, a very broad (almost double) minimum is observed, and the slopes E_{a0} of T_1 and T_2 versus $1/T$ are much lower than in ZrV_2H_4 and contrary to the concentration dependence of E_{a0} up to $x=4$. This observation supports the indications that $x=4$ is a quasi-stoichiometric composition. As mentioned above, recent neutron scattering investigations of $\text{ZrV}_2\text{D}_{3.6}$ and HfV_2D_4 indicated random occupation of alternate (nonadjacent) e

and g sites above 300 K and formation of a superstructure of protons occupying mostly analogs of the g sites in a tetrahedral structure below 280 K.^{12,13} In addition, V^{51} nuclear quadrupole resonance (NQR) of ZrV_2H_x also indicated low-temperature "crystallization" of an ordered proton sublattice for $x=4$ but none at lower concentrations.⁹ It therefore appears from Fig. 12 that additional protons beyond this quasistoichiometric concentration thwart the formation of this superstructure and enhance hydrogen diffusion.

V. DISCUSSION AND SUMMARY

One of the major results of this work is the validity of the Zener relation, i.e., the linear relation between the logarithm of the preexponential and the activation energy (enthalpy of motion). A phenomenological derivation of the relation was given by Wert and Zener²⁰ (later derived from a quantum theory of diffusion developed by Flynn and Stoneham²²) a long time ago, and is briefly repeated here. In case of interstitial diffusion one would expect

$$A_0 = \nu_{00} e^{\Delta S/k} \quad (16)$$

Here $\nu_{00} = n\nu$, where n is the number of nearest-neighbor interstitial positions ($n=3$ for the g site in the cubic C15 Laves phase), and ν is the vibration frequency of the proton in the site. ΔS is the activation entropy (the entropy difference involved in displacing a proton from the interstitial site to the "saddle point" position). The activation free energy ΔF is obviously given by

$$\Delta F = \Delta H - T \Delta S = E_a - T \Delta S \quad (17)$$

In case of interstitial diffusion, if all of the free energy required for the hopping process goes into straining the lattice, and E_a and ΔS are temperature independent, then^{20,21}

$$\Delta S = E_a \frac{d(\mu/\mu_0)}{dT} \quad (18)$$

Here μ is an appropriate elastic shear modulus and $\mu_0 = \mu(T=0 \text{ K})$. Substitution of Eq. (18) in (16) immediately results in the Zener relation, and β is then the temperature derivative of the relative shear modulus

$$\beta = \frac{d(\mu/\mu_0)}{dT} \quad (19)$$

The Zener relation has been observed in the diffusion of various dilute interstitials in simple metals,²⁰ and in the hydride systems $LaNi_{5+x}H_{6+y}$ ($x, y \geq 0$), $LaNi_{5-x}Cu_xH_y$, $LaNi_{5-x}Al_xH_y$,²⁸ and amorphous $Pd_{77.5}Cu_6Si_{16.5}H_x$.²⁹ In all of these hydride systems, the slope β of $\ln \nu_0$ versus E_{a0} is $\beta = (3 \pm 1) \times 10^{-3} \text{ K}^{-1}$. Yet in these intermetallic hydrides β is an order of magnitude larger than in most of the elemental metals.²⁰ At present it is difficult to explain this difference: Possibly the temperature derivatives of the elastic shear moduli of these intermetallics are indeed much larger than those of the simple metals (which may perhaps hint to the nature of the difference in the mechanical properties, i.e., the intermetallics being generally much more brittle). Another possibility is that the

large value of β is related to the small value of ν_{00} (see below).

In an earlier work, it was suggested that the linear relation between $\ln \nu_0$ and E_{a0} may originate from a temperature-dependent activation energy resulting from thermal expansion.²⁸ At present it is difficult to rule out the possibility that a temperature-dependent E_{a0} contributes to the linear relation between $\ln A_0$ and E_{a0} . However, that contribution cannot be the dominant one, otherwise it would lead to negative activation energies at high temperatures. Finally, it should be noted that a significant dependence of ΔS on temperature would probably result in a hopping-rate behavior which is qualitatively different from an Arrhenius one.

Another problem associated with the observation of the Zener relation in the HfV_2H_x and ZrV_2H_x systems is the small value of ν_{00} , about 10^9 sec^{-1} . As mentioned in Sec. IV, the usual interpretation of ν_{00} as $n\nu$ is obviously unacceptable, since the proton vibrational frequency is expected to be of order 10^{12} – 10^{13} sec^{-1} . Although the same value of A_0 may be obtained from a given value of E_a by simultaneously increasing ν_{00} and decreasing β , this solution to the problem of the values of β and ν_{00} is improbable for several reasons. (a) A substantial reduction of β would again produce an effectively E_a -independent A_0 . This is contrary to the behavior of T_1 and T_2 observed in several concentrations (especially in e.g., $ZrV_2H_{1.5}$ and $HfV_2H_{2.5}$ (Figs. 6 and 9)). (b) Regardless of the specific dependence of A_0 on E_a within each concentration, the dependence of the average preexponential on the average activation energy, among the various concentrations, is still given by the Zener relation, with the above (anomalous) values of β and ν_{00} (see Sec. IV B above). (c) As mentioned above, the Zener relation is also observed in other ternary and quaternary metal-hydrogen systems,^{28,29} with similar values of ν_{00} and β . (d) Anomalously low values of the preexponential A_0 have been observed previously in many cases of chemical diffusion (but not self-diffusion) in metals.²⁷ The small values of A_0 were invariably coupled to small values of E_a , thus retaining the Zener relation between them. In this context, it should be noted that the values of E_{a0} in HfV_2H_x and ZrV_2H_x are surprisingly low (1000–2000 K) at hydrogen concentrations $x \leq 2$, considering the large (exothermic) heat of reaction between the H_2 gas and the intermetallic compound and the resulting stability of the hydrides.^{2,4,5}

A possible explanation of the observed low values of E_a , suggested recently,^{30,31} involves appropriate diffusion paths believed to result from lattice inhomogeneities created earlier by static distortions (as in amorphous systems^{30,31}) or by large local concentration gradients. Indeed, Richards³¹ has shown that in amorphous systems one would expect the average activation energy to be determined by the area of the largest face of the distorted tetrahedral or octahedral interstitial site. Since the largest face is, on the average, larger than that of the analogous ordered structure, this would lead to a reduced average activation energy in the distorted system. Bowman's observations of the hopping rates in a -TiCu and a -Zr₂Pd hydrides, which are greatly enhanced (and governed by con-

siderably lower activation energies) relative to the ordered structures, are in complete qualitative agreement with these concepts. The rapid rise of E_{a0} [and with it $v_0 = v_{00} \exp(\beta E_{a0})$] with concentration x in HfV_2H_x and ZrV_2H_x (see Table I and Fig. 13) may now be explained as resulting from the host metal lattice becoming more and more homogeneous as hydrogen is added, until the quasi-stoichiometric concentration $x = 4$ is reached. When the lattice resumes its distorted nature above $x = 4$, E_{a0} decreases to a lower value [see the behavior of T_1 and T_2 in $\text{ZrV}_2\text{H}_{4.2}$ (Fig. 12)].

The suggestion that lattice inhomogeneities play a crucial role in the hydrogen diffusion properties in HfV_2H_2 and ZrV_2H_x lends added support to the assumption of a non-negligible distribution of activation energies. This brings us to the second major feature of this work, namely the analysis of the relaxation rates in terms of such a distribution. The telltale marks of diffusion governed by a distribution of activation energies are the asymmetric slopes of $\ln T_1$ versus $1/T$ and the flattening of $\ln T_1$ versus $1/T$ at low temperatures, features observed more often than not in disordered systems of various kinds: hydrides,^{30,32,33} fast ion conductors,^{19,34} and amorphous metal-hydrogen systems.³⁵ A final mark of diffusion

governed by a distribution of E_a 's observed in this work is the "bending downward" of $\ln T_2$ versus $1/T$ (as mentioned above and seen in Figs. 3, 4, 6, and 7). Indeed this mark of a distribution of E_a 's is more unambiguous than the behavior of $\ln T_1$: Asymmetric slopes and flattening of $\ln T_1$ also appear when the (unique) activation energy decreases to lower values at low temperatures. However, in that case the slope of $\ln T_2$ versus $1/T$ decreases at low temperatures, i.e., a behavior opposite to that observed in HfV_2H_x and ZrV_2H_x .

ACKNOWLEDGMENTS

We are deeply grateful to Professor N. Kaplan for encouraging this work, for various discussions, as well as for the use of the 33-MHz spectrometer in Jerusalem. We wish to thank also Professor E. Ehrenfreund for the use of and assistance with the spectrometer at the Technion. This work was supported in part by a grant from the National Council for Research and Development (Israel) and the Kernforschungsanlage, Jülich (Germany). One of us (D.S.) would like to thank the Hebrew University Research Center for Hydrogen and Redox Fuels Synthesis, Utilization and Storage, for partial financial support.

- ¹R. L. Beck, Denver Research Institute Summary Report No. DRI-2059, 1962 (unpublished).
- ²A. Pebler and E. A. Gulbransen, *Trans. Metall. Soc. AIME* **239**, 1593 (1967).
- ³J. J. Reilly and R. H. Wiswall, *Inorg. Chem.* **6**, 2220 (1967); **7**, 2254 (1968); **13**, 218 (1974). Also K. Yamanaka, H. Saito, and M. Someno, translated from *Nippon Kagaku Kaishi* **8**, 1267 (1975).
- ⁴F. A. Kuijpers, *Phillips Res. Rep. Suppl.* **2** (1973); H. H. Van Mal, *ibid.* **1** (1976).
- ⁵D. Shaltiel, I. Jacob, and D. Davidov, *J. Less-Common Met.* **53**, 117 (1977); D. Shaltiel, *ibid.* **62**, 407 (1978); J. Shinar, D. Shaltiel, D. Davidov, and A. Grayevsky, *ibid.* **60**, 209 (1978).
- ⁶H. W. Newkirk, A Literature Survey of Metallic Ternary and Quaternary Hydrides, Report No. UCRI-51244, 1974 (unpublished).
- ⁷E. R. Bauminger, D. Davidov, I. Felner, I. Novik, S. Ofer, and D. Shaltiel, *Physica* **86-88B**, 201 (1977).
- ⁸V. U. S. Rao, D. M. Gualtieri, S. Krishnamurthy, A. Patkin, and P. Duffer, *Phys. Lett.* **67A**, 223 (1978).
- ⁹M. Peretz, J. Barak, D. Zamir, and J. Shinar, *Phys. Rev. B* **23**, 1031 (1981).
- ¹⁰D. T. Ding, J. I. Delange, T. O. Klassen, N. J. Poulis, D. Davidov, and J. Shinar, *Solid State Commun.* **42**, 137 (1982).
- ¹¹P. Duffer, D. M. Gualtieri, and V. U. S. Rao, *Phys. Rev. Lett.* **37**, 1410 (1976).
- ¹²J. J. Didisheim, K. Yvon, D. Shaltiel, P. Fischer, P. Bujard, and E. Walker, *Solid State Commun.* **32**, 1087 (1979); J. J. Didisheim, K. Yvon, P. Fischer, and P. Tissot, *ibid.* **38**, 637 (1981); J. J. Didisheim, K. Yvon, P. Fischer and D. Shaltiel, *J. Less-Common Met.* **73**, 355 (1980).
- ¹³A. V. Irodova, V. P. Glaskov, V. A. Somenkov, and S. Sh. Shiltein, *J. Less-Common Met.* **77**, 89 (1981).
- ¹⁴D. P. Shoemaker and C. B. Shoemaker, *J. Less-Common Met.* **68**, 43 (1979).
- ¹⁵I. Jacob, J. M. Bloch, D. Shaltiel, and D. Davidov, *Solid State Commun.* **35**, 155 (1980).
- ¹⁶A. Stern, S. R. Kreitzman, A. Resnik, D. Shaltiel, and V. Zevin, *Solid State Commun.* **40**, 837 (1981); A. Stern, A. Resnik, and D. Shaltiel, *J. Less-Common Met.* **88**, 431 (1982).
- ¹⁷N. Bloembergen, E. M. Purcell, and R. V. Round, *Phys. Rev.* **73**, 679 (1948).
- ¹⁸A. Abragam, *Principles of Nuclear Magnetism* (Oxford University Press, Oxford, 1961).
- ¹⁹R. E. Walstedt, R. Dupree, J. P. Remeika, and R. Rodriguez, *Phys. Rev. B* **15**, 3442 (1977).
- ²⁰C. Wert and C. Zener, *Phys. Rev.* **26**, 1169 (1949); C. Zener, *J. Appl. Phys.* **22**, 372 (1951).
- ²¹J. Shinar (unpublished results).
- ²²C. P. Flynn and A. M. Stoneham, *Phys. Rev. B* **1**, 3966 (1970).
- ²³H. C. Torrey, *Phys. Rev.* **92**, 962 (1953).
- ²⁴J. Shinar (unpublished results).
- ²⁵M. Peretz, D. Zamir, G. Cinader, and Z. Hadari, *J. Phys. Chem. Solids* **37**, 105 (1976).
- ²⁶S. J. Allen and J. P. Remeika, *Phys. Rev. Lett.* **33**, 1478 (1974); J. C. Wang, M. Gaffari, and S. Choi, *J. Chem. Phys.* **63**, 772 (1975).
- ²⁷A. S. Nowick, *J. Appl. Phys.* **22**, 1182 (1951).
- ²⁸J. Shinar, D. Davidov, and R. D. Hogg, *Solid State Commun.* **37**, 175 (1981); **40**, 645 (1981).
- ²⁹R. Kirchheim, F. Sommer, and G. Schluckebier, *Acta Metall.* **30**, 1059 (1980); **30**, 1069 (1980).
- ³⁰R. C. Bowman, A. J. Maeland, and W. K. Rhim, *Phys. Rev. B* **26**, 6362 (1982); R. C. Bowman, Jr., A. Attalla, A. J. Maeland, and W. L. Johnson, *Solid State Commun.* **47**, 779 (1983).
- ³¹P. M. Richards, *Phys. Rev. B* **27**, 2059 (1983).
- ³²T. K. Halstead, N. A. Abood, and K. H. J. Buschow, *Solid State Commun.* **19**, 425 (1976).
- ³³T. C. Jones, T. K. Halstead, and K. H. J. Buschow, *J. Less-Common Met.* **73**, 209 (1980).
- ³⁴K. L. Ngai, *Solid State Ionics* **5**, 27 (1981).
- ³⁵B. S. Berry and W. C. Pritchett, *Phys. Rev. B* **24**, 2299 (1981).